

## Accepted Manuscript

Seasonal and interannual variability of dissolved oxygen around the Balearic Islands from hydrographic data

R. Balbín, J.L. López-Jurado, A. Aparicio-González, M. Serra

PII: S0924-7963(13)00309-6  
DOI: doi: [10.1016/j.jmarsys.2013.12.007](https://doi.org/10.1016/j.jmarsys.2013.12.007)  
Reference: MARSYS 2468

To appear in: *Journal of Marine Systems*

Received date: 22 February 2013  
Revised date: 18 December 2013  
Accepted date: 25 December 2013



Please cite this article as: Balbín, R., López-Jurado, J.L., Aparicio-González, A., Serra, M., Seasonal and interannual variability of dissolved oxygen around the Balearic Islands from hydrographic data, *Journal of Marine Systems* (2014), doi: [10.1016/j.jmarsys.2013.12.007](https://doi.org/10.1016/j.jmarsys.2013.12.007)

This is a PDF file of an unedited manuscript that has been accepted for publication. As a service to our customers we are providing this early version of the manuscript. The manuscript will undergo copyediting, typesetting, and review of the resulting proof before it is published in its final form. Please note that during the production process errors may be discovered which could affect the content, and all legal disclaimers that apply to the journal pertain.

# Seasonal and interannual variability of dissolved oxygen around the Balearic Islands from hydrographic data

R. Balbín, J.L. López-Jurado, A. Aparicio-González, M. Serra

*Instituto Español de Oceanografía, Centro Oceanográfico de Baleares, Palma de Mallorca, Spain*

---

## Abstract

Oceanographic data obtained between 2001 and 2011 by the Spanish Institute of Oceanography (IEO, Spain) have been used to characterise the spatial distribution and the temporal variability of the dissolved oxygen around the Balearic Islands (Mediterranean Sea). The study area includes most of the Western Mediterranean Sea, from the Alboran Sea to Cape Creus, at the border between France and Spain. Dissolved Oxygen (DO) at the water surface is found to be in a state of equilibrium exchange with the atmosphere. In the spring and summer a subsurface oxygen supersaturation is observed due to the biological activity, above the subsurface fluorescence maximum. Minimum observed values of dissolved oxygen are related to the Levantine Intermediate Waters (LIW). An unusual minimum of dissolved oxygen concentrations were also recorded in the Alboran Sea Oxygen Minimum Zone. The Western Mediterranean Deep Waters (WMDW) and the Western Intermediate Waters (WIW) show higher values of dissolved oxygen than the Levantine Intermediate Waters due to their more recent formation. Using

---

*Email address: rosa.balbin@ba.ieo.es* (R. Balbín)

these dissolved oxygen concentrations it is possible to show that the Western Intermediate Waters move southwards across the Ibiza Channel and the deep water circulates around the Balearic Islands. It has also been possible to characterise the seasonal evolution of the different water masses and their dissolved oxygen content in a station in the Algerian sub-basin.

*Keywords:* Ocean circulation, dissolved oxygen, water masses, Western Mediterranean Sea, Balearic Sea

---

## 1 **1. Introduction**

2 The Balearic Islands are the natural limit present between two sub-basins  
3 of the Western Mediterranean Sea, viz., the Algerian and Balearic sub-basins  
4 (Fig. 1). The Algerian sub-basin receives fresh surface water from the At-  
5 lantic Ocean (Atlantic Water, AW), and its circulation is mainly driven by  
6 density gradients. The Balearic sub-basin contains the colder and saltier AW  
7 that has remained for a longer time in the Mediterranean (resident AW), and  
8 its circulation is affected by atmospheric forcing (Hopkins, 1978). The Ma-  
9 llorca and Ibiza channels play an important role in the regional circulation  
10 of the water masses in the area. Their topography controls the exchanges  
11 between the two sub-basins (Pinot et al., 2002). Consequently, significant dif-  
12 ferences are visible between the general hydrodynamic conditions that affect  
13 the northern and the southern regions of the Balearic Islands. The confluence  
14 of the fresher and resident surface AW around the Balearic Islands triggers  
15 ocean fronts that affect the dynamics (López-García et al., 1994; Balbín et al.,  
16 2013).

17 Two intermediate waters are present surrounding the Balearic Islands,

18 viz., the Levantine Intermediate Water (LIW) and the Western Intermediate  
19 Water (WIW). The LIW, formed in the Eastern Mediterranean Sea, is char-  
20 acterised by an absolute maximum of salinity, a relative maximum of temper-  
21 ature and an absolute minimum of dissolved oxygen (DO). The WIW, on the  
22 other hand, is formed seasonally during the winter convection processes in  
23 the Gulf of Lions over the continental shelf extending from the Ligurian Sea  
24 to the Ebro Delta (Vargas-Yáñez et al., 2012). The WIW lies above the LIW,  
25 and varies in thickness from tens to a few hundred metres. It is characterised  
26 by an absolute minimum of temperature and shows relative high values of  
27 DO. Just below the WIW and LIW lies the Western Mediterranean Deep  
28 Water (WMDW), formed during the deep winter convection events in the  
29 Gulf of Lions and the Ligurian Sea (MEDOC-Group, 1970). Table 1 shows  
30 the salinity,  $S$  and potential temperature,  $\theta$ , that characterise the different  
31 water masses and their values in the area, after López-Jurado et al. (2008);  
32 Table 2 shows the spatially averaged water properties in the Gulf of Lions  
33 and the Alboran Sea after Manca et al. (2004). The intermediate and deep  
34 water masses reach the Balearic channels after circulating along the conti-  
35 nental slope of the north western Mediterranean. The WIW is dragged by  
36 the Northern Current (NC) into the Gulf of Valencia and the Ibiza channel  
37 towards the end of the winter and until the beginning of the spring, although  
38 it is not found in the Balearic channels every year (López-Jurado et al., 2008).

39 The vertical and horizontal distributions of the DO in the oceans reflect  
40 a balance between the exchange across the air-sea interface with the atmo-  
41 sphere, its involvement in the biological and chemical processes and its phys-  
42 ical transport. Oxygen solubility is strongly temperature dependent and de-

43 creases at higher temperatures. Within the mixed layer, the DO very closely  
44 approaches the temperature-dependent saturation concentration. The oxy-  
45 gen solubility lowest concentrations are reached during late summer, while  
46 the highest are seen in late winter (Najjar and Keeling, 1997).

47 At the sub-surface level, the atmospheric supply is supplemented by the  
48 oxygen released during the photosynthetic processes occurring in the photic  
49 zone (Chester, 2000). As photosynthesis can produce a DO supersaturation,  
50 a shallow DO maximum has been reported in some oligotrophic marine re-  
51 gions like the Mediterranean Sea (e.g. Deya-Serra, 1978; Manca et al., 2004).  
52 On the contrary, the sub-surface DO minima are a common feature found in  
53 many productive regions, particularly in the non-oligotrophic regions. Below  
54 the euphotic depth a decrease in DO is observed due to consumption by the  
55 respiration and remineralization of organic matter.

56 Oxygen minima are a characteristic feature of many marine areas and  
57 are due to an *in situ* consumption of oxygen or to less oxygenated waters  
58 advected into the area. One example is the DO minimum zone (OMZ) in the  
59 Alboran Sea related to the LIW core (Packard et al., 1988) or the OMZs of the  
60 tropical Atlantic and the equatorial Pacific (Stramma et al., 2008). There  
61 is a small amount of oxygen consumption in the deep waters. Therefore,  
62 the DO distribution has been used as a non-conservative tracer to identify  
63 the pathway of water masses around the ocean basins or to qualitatively  
64 indicate its age, defined as the time elapsed since the fluid was at the surface  
65 (Jenkins, 1987). In practice, a quantitative calculation of the age from the  
66 DO concentrations is rarely performed, as it requires assumptions to be made  
67 regarding the consumption of oxygen, along with the exact paths of the fluid

68 parcels and interior mixing (Stratford et al., 1998).

69 The objective of this work is to describe the spatial distribution and  
70 seasonal and interannual behaviour of the DO around the Balearic Islands.  
71 Keeping this aim in focus, after presenting the available data, we will first  
72 describe the spatial distribution of the DO along the Spanish Mediterranean  
73 Coast followed by a discussion of the main features of the DO in the dif-  
74 ferent water masses and their seasonal evolution, computing the seasonal  
75 mean values at four representative positions around the Balearic Islands.  
76 The interannual variability of the DO at the different water masses will be  
77 discussed using the data obtained from a deep station at Cape Palos between  
78 the summer of 2007 and the autumn of 2011. Finally, the seasonal evolution  
79 of dissolved oxygen of biological origin will be considered.

## 80 **2. Material and methods**

81 The data used in this study were obtained over the course of several  
82 projects developed by the Spanish Institute of Oceanography (IEO) and are  
83 compiled under the IBAMar database (Aparicio et al., 2012). The spatial  
84 coverage extends from the Alboran Sea to Cape Creus, including the Balearic  
85 Islands. The period used in this study extends from 2001 to 2011 and the data  
86 correspond to the following projects, viz., TUNIBAL (Alemany et al., 2010),  
87 IDEA (López-Jurado et al., 2008), IDEADOS (Massutí et al., 2013), CIRBAL  
88 and RADMED (Amengual et al., 2010), which had been developed within  
89 the area using a similar strategy and methodology for the data collection.  
90 This spatiotemporal range facilitates the observation of the differences in the  
91 spatial and temporal distribution of the DO content in the different water

92 masses.

93 The dissolved O<sub>2</sub> concentration measured will hereafter be referred to as  
94 DO. The hydrographic data were recorded using different CTDs, SBE911 and  
95 SBE25, operating at a sampling rate of 24 and 8 Hz, respectively. A SBE43  
96 sensor with a redesign of a Clark polarographic membrane was used to record  
97 the DO. The CTDs were lowered at an average speed of less than 1 m s<sup>-1</sup>.  
98 The salinity ( $S$ ), potential temperature ( $\theta$ ) and the DO were processed using  
99 the Sea-Bird Electronics Data Processing routines. The salinity and DO  
100 concentration were calibrated on board using the water samples, whenever  
101 available. The DO determinations were performed by the Winkler titration  
102 method (Strickland and Parsons, 1972). The water samples were available  
103 when the SBE911 with a Rosetta was used (70 % of the cases presented  
104 in this work). Calibration was performed for selected depths of the water  
105 column at least once, when the campaign was less than a week, and done at  
106 least at the beginning and at the end of the campaign, when it was longer.  
107 During the TUNIBAL campaigns, the calibrations were done every three  
108 days. The spare SBE25 were cross-calibrated with a SBE911 and Rosetta at  
109 least once every campaign. Under extreme pressure, changes can occur in  
110 the gas permeable membranes which affect their permeability characteristics.  
111 Some of these changes have long-term constants and depend upon the sensors  
112 time-pressure history. These slow processes result in hysteresis in long, deep  
113 casts. Strictly following the SBE recommendations it is possible to correct  
114 this effect (SBE43, 2013). When the Rosetta samples were not available, the  
115 potential drift with time in the SBE43 was estimated using the previous and  
116 posterior campaign calibrations. Taking into account the sensor evolution

117 between the campaigns and the available calibrations, the DO uncertainty  
118 is estimated to be  $0.1 \text{ ml l}^{-1}$ . Although the DO units of  $\mu\text{mol kg}^{-1}$  are  
119 often used in oceanography, the results will be presented in  $\text{ml l}^{-1}$  to help the  
120 comparison with the available climatologies (Manca et al., 2004) and previous  
121 works (Miller, 1970; Packard et al., 1988; Garcia et al., 2006). Conversion  
122 from  $\text{ml l}^{-1}$  to  $\mu\text{mol kg}^{-1}$  is easily done using the water density available  
123 (SBE43, 2013).

124 The  $\text{O}_2$  gas solubility,  $\text{O}_2^*$ , is the  $\text{O}_2$  concentration ( $\text{ml l}^{-1}$ ) calculated  
125 as a function of *in situ* temperature and salinity, at atmospheric pressure.  
126 The  $\text{O}_2^*$  values were calculated using the SBE routines (SBE43, 2013; Garcia  
127 and Gordon, 1993). The oxygen saturation,  $\text{O}_2^S$  (%), was calculated as the  
128 percentage of the DO over  $\text{O}_2^*$ . Apparent Oxygen Utilisation, AOU ( $\text{ml l}^{-1}$ ),  
129 was calculated as  $\text{O}_2^* - \text{DO}$ . The AOU is an estimate of the  $\text{O}_2$  utilised due  
130 to biochemical processes relative to the solubility value (Garcia et al., 2006)  
131 and may be more informative regarding the age of the water mass.

132 Fluorescence data, obtained with a WET Labs ECO fluorometer, provide  
133 an indication of the chlorophyll- $\alpha$  concentration (Cullen, 1982). It will also be  
134 shown, if available and if it helps the discussion, without any calibration but  
135 with an offset correction (one for each campaign) to achieve zero fluorescence  
136 level at 1000 to 1500 dbar.

137 One of the aims of this study is to highlight the evolution of the DO con-  
138 tent in the different water masses, along their path in the Western Mediter-  
139 ranean basin. Therefore, the study is focused on those hydrographic stations  
140 that have been visited more often, ensuring that their distribution was rep-  
141 resentative of the whole study area and reached the deep waters.



### 142 3. Results

143 The RADMED-1007 campaign conducted during October 2007 is used  
144 to characterise the DO distribution along the Mediterranean Spanish coast,  
145 from Barcelona to Gibraltar. This particular campaign was chosen because  
146 all the deep stations were visited and  $S$ ,  $\theta$  and DO are all available. The  
147 station locations are shown in Fig. 2. The stations selected are at Barcelona  
148 (115), Ibiza channel (25 and 16), Cape Palos (145), Cape Gata (155), Sacratif  
149 (165), Málaga (185) and Cape Pino (194). Fig. 3 shows the DO and vertical  
150 profiles of fluorescence of the stations selected, together with their  $\theta - S$   
151 diagrams. The surface values are not shown in the  $\theta - S$  diagram. The  
152 maximum DO values,  $\approx 5.8 \text{ ml l}^{-1}$  ( $\text{AOU} \approx -0.5 \text{ ml l}^{-1}$ ,  $\text{O}_2^S \approx 111 \%$ ) at  $\approx$   
153 50 dbar correspond to stations 25 and 16 in the Ibiza channel. The vertical  
154 profiles of temperature, not displayed, reflect a surface mixed layer between  
155 10 dbar and 20 dbar and a thermocline of temperature decreasing from  $\approx 18$   
156  $^\circ\text{C}$  to  $22 \text{ }^\circ\text{C}$  at 20 dbar to  $\approx 14 \text{ }^\circ\text{C}$  at 100 dbar. The minimum DO values  
157 oscillate between  $\approx 4.0 \text{ ml l}^{-1}$  ( $\text{AOU} \approx 1.8 \text{ ml l}^{-1}$ ,  $\text{O}_2^S \approx 70 \%$ ) at station  
158 115 (Barcelona) and  $\approx 3.2 \text{ ml l}^{-1}$  ( $\text{AOU} \approx 2.6 \text{ ml l}^{-1}$ ,  $\text{O}_2^S \approx 55 \%$ ) at station  
159 194 (Cape Pino, in the Alboran sea) between the 300 to 600 dbar, around  
160 the LIW core, shown in the  $\theta - S$  diagrams. The DO values increase at  
161 depths corresponding to the deep waters, and oscillate between  $\approx 4.5 \text{ ml l}^{-1}$   
162 ( $\text{AOU} \approx 1.3 \text{ ml l}^{-1}$ ,  $\text{O}_2^S \approx 78 \%$ ) in station 115 (Barcelona) and  $\approx 4.3 \text{ ml}$   
163  $\text{l}^{-1}$  ( $\text{AOU} \approx 1.5 \text{ ml l}^{-1}$ ,  $\text{O}_2^S \approx 74 \%$ ) in station 145. The fluorescence profiles  
164 show a subsurface fluorescence maxima at  $\approx 60$  dbar 70 dbar, indicating  
165 the presence of a deep chlorophyll- $\alpha$  maximum, DCM (Estrada, 1996), in all  
166 the stations, except for stations 185 and 194 in the Alboran sea, where the

167 maximum fluorescence values reach the surface.

168 Fig. 4 shows the vertical profiles of the DO and AOU data from three  
169 IDEA campaigns, Idea0204 (winter), Idea0404 (spring) and Idea0604 (sum-  
170 mer) and their corresponding  $\theta - S$  diagrams. To characterise the possible  
171 differences between the Balearic and the Algerian sub-basins, black lines are  
172 used to indicate stations 34 to 45 (north of the sampling area) and grey lines  
173 are employed to show stations 1 to 17 (south of the sampling area) as seen  
174 in the map. Table 3 shows a summary of the  $O_2^S$  and AOU values calculated  
175 for this Fig. at the depths corresponding to the different water masses.

176 During Idea0204, corresponding to February 2004, the surface DO values  
177 are seen to be close to saturation  $\approx 5.6 \text{ ml l}^{-1}$ . Below the surface, between  
178 80 dbar and 130 dbar the relative DO maxima are also close to saturation  
179 values. At  $\approx 500$  dbar there are absolute DO minima,  $\approx 3.8 \text{ ml l}^{-1}$ , while  
180 at the bottom the DO values observed are slightly increased showing  $\approx 4.2$   
181  $\text{ml l}^{-1}$  in the Balearic sub-basin and  $\approx 4.0 \text{ ml l}^{-1}$  in the Algerian one. The  
182  $\theta - S$  diagrams for Idea0204 show the absence of WIW in the region sam-  
183 pled, although some possible episodes of intermediate convection appear as  
184 a sudden  $\theta$  reduction (up to  $\approx 0.3 \text{ }^\circ\text{C}$ ) in the different stations, mainly in the  
185 Balearic sub-basin (black lines).

186 The Idea0404 campaign, occurring during April 2004, shows surface DO  
187 values that reach saturation  $\approx 5.5 \text{ ml l}^{-1}$ . Below the surface at around 150  
188 dbar relative DO maxima of  $\approx 5.3 \text{ ml l}^{-1}$  are noted. Between 400 dbar and  
189 500 dbar absolute DO minima of  $\approx 3.9 \text{ ml l}^{-1}$  are seen, and at the bottom,  
190 the DO show values of  $\approx 4.1 \text{ ml l}^{-1}$  in the Balearic sub-basin. The  $\theta - S$   
191 diagrams for Idea0404 show the absence of the WIW in the region sampled,

192 strictly considering the  $\theta$  and  $S$  ranges, although the scattered episodes of  
193 intermediate water formation accumulate water showing  $\theta$  values slightly  
194 above 13 °C, very close to the ranges that characterise the WIW in the area.

195 Finally, the Idea0604 campaign, running during June 2004, shows the  
196 surface DO values that reach saturation  $\approx 4.8 \text{ ml l}^{-1}$  and a sub-surface value  
197 of  $\approx 40 \text{ dbar}$ , with supersaturation up to  $\approx 6.3 \text{ ml l}^{-1}$ . Below the surface, at  
198 around 150 dbar, relative DO maxima of  $\approx 5.1 \text{ ml l}^{-1}$  are seen. Between 400  
199 dbar and 500 dbar there are absolute DO minima of  $\approx 3.9 \text{ ml l}^{-1}$ , while close  
200 to the bottom the DO show values of  $\approx 4.1 \text{ ml l}^{-1}$  in both the Balearic and  
201 the Algerian subbasins. The  $\theta - S$  diagrams for Idea0604 show the presence  
202 of WIW in both the sub-basins revealing  $\theta$  below 13 °C.

203 Using the IBAMar database it was possible to compute the seasonal mean  
204 values of  $\theta$ ,  $S$ , DO and AOU at four reference points: the Menorca deep  
205 station, to characterise the Provençal sub-basin (station 88 in Fig. 2), the  
206 Cabrera deep station for the Algerian sub-basin (station 66 in Fig. 2), and  
207 the Ibiza and the Mallorca channels. These two describe the interchanges  
208 between the Balearic and Algerian sub-basins (stations 25 and 33 in Fig.  
209 2). The mean values were calculated using the data from campaigns running  
210 from October 2001 to October 2011. The curves shown in Fig. 5 are a mean  
211 value of at least three vertical profiles, in winter, and up to 20, in spring and  
212 summer. The Fig. shows the vertical profiles of the AOU mean values at  
213 the stations selected for winter, spring, summer and autumn and their  $\theta - S$   
214 diagrams.

215 In Fig. 6 the horizontal sections of the DO at 400 m, around the LIW  
216 core depth, and at 800 m depth, about the interface with the DWs are shown.

217 The plots correspond to December 2009 and June 2010 IDEADOS surveys.  
218 During December 2009, the north DO values are around  $4.20 \text{ ml l}^{-1}$  and  
219  $4.37 \text{ ml l}^{-1}$  at 400 m and 800 m, respectively, while the south DO values are  
220 around  $4.05 \text{ ml l}^{-1}$  and  $4.27 \text{ ml l}^{-1}$  at 400 m and 800 m, respectively. During  
221 June 2010, the north DO values are around  $4.05 \text{ ml l}^{-1}$  and  $4.27 \text{ ml l}^{-1}$  at  
222 400 m and 800 m, respectively, while the south DO values are around  $4.05$   
223  $\text{ml l}^{-1}$  and  $4.20 \text{ ml l}^{-1}$  at 400m and 800m, respectively.

224 Cape Palos (RADMED stations 143 and 144 in Fig. 2) has been chosen  
225 to characterise the seasonal evolution of the AOU cycle in the intermediate  
226 and deep waters (Figs. 7 and 8) because it has a stable circulation pattern.  
227 It is found in the Algerian sub-basin, far away from the areas of WMDW and  
228 WIW formation, a fact that helps to smooth out the strong seasonal variability  
229 observed in the formation events in the Balearic sub-basin. Cape Palos  
230 was sampled every season (every three to four months), from the summer of  
231 2007 to the autumn of 2011. The data include the potential temperature ( $\theta$ ),  
232 salinity ( $S$ ), AOU and potential density ( $\sigma_\theta$ ). When the interest focuses on  
233 the surface and intermediate waters, station 143 is used for clarity, because  
234 more AOU data are available there, although the results are similar for both  
235 stations. In Fig. 7 the variables are plotted from the surface to 500 dbar  
236 and down to 2000 dbar in Fig. 8. To smooth the high frequency oscillations,  
237 data were interpolated into a regular grid every 15 dbar and 45 days.

238 In Fig. 9 the annual cycle of  $\text{O}_2^S$  and fluorescence from 0 to 150 dbar,  
239 using the IBAMar database are seen. The stations have been chosen to lie  
240 between longitude  $1^\circ\text{E}$  and  $5^\circ\text{E}$  and latitude  $38^\circ\text{N}$  and  $45^\circ\text{N}$ . Only stations  
241 with a bottom depth greater than 300 m were considered, to avoid coastal

242 effects. Although more than 1400 stations exist within these requirements  
243 no data is available from the middle of December to the middle of February.  
244 To smooth the statistical oscillations, data were interpolated into a regular  
245 grid every 5 dbar and 5 days. The fluorescence around the Balearic Islands  
246 is observed to be very patchy. Although some (very few) stations do exhibit  
247 a fluorescence maxima up to  $8 \text{ mg m}^{-3}$  the smoothed signal maximum values  
248 hover around  $1 \text{ mg m}^{-3}$ .

## 249 4. Discussion

### 250 4.1. Spatial distribution of dissolved oxygen (DO) along the Spanish Mediter- 251 ranean Coast

252 Vertical profiles of DO (Fig. 3) show the presence of a subsurface ( $\approx 50$   
253 dbar) maximum of up to  $5.8 \text{ ml l}^{-1}$  ( $\text{AOU} \approx -0.5 \text{ ml l}^{-1}$ ,  $\text{O}_2^S \approx 111 \%$ ) in all  
254 the stations except 194 and 185 in the Alboran sea. This maximum is within  
255 the thermocline (from 20 to 100 dbar) and appears  $\approx 10$  dbar 20 dbar above  
256 the DCM. There is no exchange with the atmosphere due to the strong strat-  
257 ification, and the supersaturation therefore is due to the biological activity  
258 (e.g Deya-Serra, 1978). Stations 194 and 185 show a surface maximum of  
259 fluorescence, related to the phytoplankton blooms usually observed, due to  
260 wind driven upwelling events in this area. In those stations, the sub-surface  
261 DO maximum, related to the DCM, is not observed because there probably  
262 is a net flux of DO of biological origin from the sea into the atmosphere.

263 At 400 dbar, a clear DO minimum is observed corresponding to the LIW  
264 core (see Tables 1 and 2). The values of DO observed at the LIW are  $\approx 0.5$   
265  $\text{ml l}^{-1}$  to  $0.8 \text{ ml l}^{-1}$  lower than the climatological values reported by Manca

266 et al. (2004). Below the LIW, the WMDW show a relative increase in the  
267 DO corresponding to the incorporation of the recently formed DW.

268 The LIW and WMDW values of DO clearly decrease from Barcelona to  
269 Gibraltar. This reduction is in agreement with the DO depletion during the  
270 remineralisation of the organic matter at greater depths in the water column  
271 (Chester, 2000) combined with the southward advection of the intermediate  
272 and deep waters along the continental shelf (Millot and Taupier-Letage, 2005).  
273 This is an indication of the increasing age of the intermediate and deep water  
274 masses as they progress southwards. Font (1987) indicates that the winter  
275 velocities in the intermediate layer are in the order of  $5 \text{ cm s}^{-1}$  and he argues  
276 that if this velocity were maintained the whole year through, the LIW would  
277 cross the Balearic Sea in about three months, and the LIW outflow through  
278 the Ibiza sill would reach the Alboran Sea two months later. If it is assumed  
279 that those velocity values are maintained constant during the year, that the  
280 LIW path is well determined along the continental slope and that there are  
281 no significant vertical mixing effects, the oxygen consumption rates would  
282 be of the order of  $1\text{-}2 \text{ ml l}^{-1} \text{ yr}^{-1}$  (from the AOU reduction observed in  
283 Fig. 3) which is much higher than the values reported for the Mediterranean  
284 (e.g. Souvermezoglou et al., 2002). This enables us to conclude that any of  
285 the hypotheses mentioned earlier are inaccurate. Therefore, it is reasonable  
286 to argue that the LIW velocity does not remain constant throughout the  
287 year and that the LIW which arrives at the Alboran Sea does not follow  
288 well-defined paths and probably the advection time is longer than the values  
289 deduced by Font (1987).

290 Oxygen Minimum Zones (OMZ) can be big phenomena. Packard et al.

291 (1988) suggested that the OMZ observed in the Alboran Sea is the result of a  
292 chain of processes, commencing with the nutrient enrichment of the Atlantic  
293 water flowing into the Mediterranean, increased by the nutrient rich water  
294 that rises by upwelling along the Spanish coast where the phytoplankton  
295 blooms occur. The blooms are transported to the convergence zone in the  
296 centre of the Alboran gyre, which acts as a plankton trap. Dead plankton  
297 and faecal material rain down into the LIW, where they are metabolised  
298 by the bacteria, a process which consumes oxygen and maintains the most  
299 intense OMZ in the Mediterranean Sea with values reported to be about 3.5  
300  $\text{ml l}^{-1}$  (Packard et al., 1988) . In Fig. 3 the minimum DO values of  $\approx 3.2$   
301  $\text{ml l}^{-1}$  in the Alboran Sea (stations 185 and 194) are shown, corresponding  
302 to the LIW core.

303 A sea surface temperature (SST) trend from 20 °C in 1985 to 21 °C in  
304 2005 has been reported in the eastern Mediterranean basin (Nykjaer et al.,  
305 2009) where the LIW is formed. This trend will decrease the oxygen solubility  
306  $\text{O}_2^*$  in the eastern basin by less than 0.1  $\text{ml l}^{-1}$ . However, this reduction  
307 in the SST is not enough to explain the DO reduction observed in the LIW  
308 in the OMZ in the Alboran Sea. Other scenarios may affect the amount of  
309 new production in the region (and therefore the DO depletion in the lower  
310 waters), such as the changing wind regimes which may change the timing,  
311 duration and intensity of the blooms, finally affecting the DO in the OMZ.  
312 More DO measurements together with the nutrients and atmospheric data  
313 are essential to clarify if the reduction in the DO observed in the Alboran  
314 OMZ is a fluctuation that occurs within the statistics, a global warming effect  
315 as has been suggested for the Atlantic and Pacific OMZs (Stramma et al.,

316 2008; Shaffer et al., 2009), an anthropogenic effect due to the increase in the  
317 nutrients in the river discharges that modify the new production (Bethoux,  
318 1989) or if it is due to other scenarios that may be induced by a modified  
319 climate (Diaz and Rosenberg, 2008).

#### 320 *4.2. Seasonal variability of dissolved oxygen around the Balearic Islands*

321 The vertical distribution of the DO around the Balearic Islands show  
322 pronounced features, related to the different water masses, which can be  
323 observed in the data presented in Fig. 4.

324 The DO in the surface layer is due to the exchange with the atmosphere  
325 and its concentration is mainly determined by the SST. Around the Balearic  
326 Islands the maximum DO values are observed at the surface in winter, when  
327 these values can be as high as 5 to 6 ml l<sup>-1</sup>. During the summer, the surface  
328 DO values are reduced by 1 to 2 ml l<sup>-1</sup>, due to the higher SST (Fig. 4  
329 Idea02014 and Idea0604). The surface DO values are close to saturation  
330 during the three Idea campaigns, as shown in Table 3. Oxygen is released  
331 during photosynthesis, although this process is restricted to the upper water  
332 column. In this area the usual limit of photosynthesis lies within the upper  
333 100 m. The exchange of photosynthetic DO with the atmosphere can be  
334 blocked due to the summer stratification with the result that the process of  
335 photosynthesis produces the oxygen supersaturation. Around the Balearic  
336 Islands this subsurface DO maximum ranges between 40 and 80 dbar and up  
337 to 6.5 ml l<sup>-1</sup> (Fig. 4 Idea0604) with O<sub>2</sub><sup>S</sup> ≈ 116 % (Table 3). Below the zone  
338 where the photosynthesis occurs, a decrease in the DO is noted owing to its  
339 biological consumption. Around the Balearic Islands this absolute minimum  
340 is observed at the core of the LIW at around 400 dbar and it is usually noted



341 to be below  $4 \text{ ml l}^{-1}$  (Fig. 4) being  $\text{O}_2^S \approx 66 \%$  constant during the three  
342 Idea campaigns (Table 3). This is probably due to the very little oxygen  
343 consumption at these depths that makes the DO appear constant during  
344 the four months sampled. The DO concentrations usually show a gradual  
345 increase from the minimum layers to the bottom of the water column. This  
346 is a result of the deep water formed during the deep convection events in  
347 winter when the surface and ventilated waters sink to the bottom. The  
348 recently formed and ventilated DW is being advected from the Gulf of Lions  
349 driving the DO increase thus observed, with depth. Once the ventilated water  
350 mass has sunk to the bottom, the DO consumption occurs by the biological  
351 activity. As this DO cannot be refilled by exchange with the atmosphere or  
352 by photosynthesis, the DO concentrations decrease with distance from the  
353 source. The deep waters are observed to present more DO to the north of  
354 the Balearic Islands than to the south in winter, (Fig. 4 Idea0204) with  
355 a difference of  $\text{O}_2^S$  of  $\approx 1 \%$  (Table 3). This difference could be due to  
356 the longer time that the WMDW needs to reach the south sampling area  
357 (grey lines) from its source along the insular slope. Amores et al. (2013)  
358 reveal average velocities from  $2$  to  $4 \text{ cm s}^{-1}$  at  $500 \text{ m}$  and from  $3$  to  $7 \text{ cm}$   
359  $\text{s}^{-1}$  at  $900 \text{ m}$ , at a mooring placed at the north sampling area, influenced  
360 by the Balearic Current, during the IDEADOS campaigns (Fig. 6). Under  
361 assumptions similar to those made to estimate the LIW consumption along  
362 the Spanish coast (Fig. 3), the oxygen consumption rates in winter will  
363 be of the order of  $0.2 \text{ ml l}^{-1} \text{ yr}^{-1}$  closer to some values reported for the  
364 Mediterranean (Souvermezoglou et al., 2002). In any case, this difference  
365 between the north and south sampling area is observed only in the winter

366 during 2004 and it could simply be due to the arrival of the more recent  
367 WMDW in the northern sampling area (Fig. 4).

368 The relative maxima of DO are also observed at around 150 dbar in  
369 the winter and spring. Each relative DO maximum corresponds to a  $\theta$   
370 reduction observed in the  $\theta - S$  diagram (Fig. 4 Idea0204 and Idea0404).  
371 Those DO maxima reflect the recently formed and ventilated intermediate  
372 water lenses that develop during different intermediate convection episodes  
373 (Vargas-Yáñez et al., 2012). In the summer profile (Fig. 4 Idea0604) only  
374 one relative maximum is noted, that appears to be due to the aggregation  
375 and homogenisation of the intermediate water lenses. The WIW is clearly  
376 observed in the corresponding  $\theta - S$  diagram.

377 The main seasonal features of the AOU can be observed in the different  
378 water masses in Fig. 5. The surface water is close to saturation,  $\text{AOU} \approx 0 \text{ ml}$   
379  $\text{l}^{-1}$ , during the four seasons. In the spring, there is a gradual increase in the  
380 temperature and the first appearance of summer subsurface oxygen super-  
381 saturation (AOU negative) due to photosynthetic activity and the beginning  
382 of stratification (Fig. 5 spring) is noted. In the summer, the DO at the  
383 surface decreases, due to the increased SST and equilibration with the atmo-  
384 sphere, although the subsurface DO maximum is reinforced due to biological  
385 activity, revealing AOU concentrations as low as  $-0.5 \text{ ml l}^{-1}$ . This AOU  
386 minimum (DO maximum) is always slightly above the DCM (not shown),  
387 (Deya-Serra, 1978), and sometimes the DO is observed to reach values up  
388 to 6 to 7  $\text{ml l}^{-1}$ . In the autumn the supersaturated structure is maintained  
389 with less intensity although in the late autumn and winter, the atmospheric  
390 forcing breaks the stratification producing a homogenisation of the surface

391 waters that equilibrate close to saturation (Fig. 5, winter). In the winter,  
392 the clear influence of the recently formed WIW is seen, with a relative AOU  
393 minimum (DO maximum) between 100 and 300 m, as is observed at station  
394 25 in the Ibiza Channel, where each relative minimum corresponds to differ-  
395 ent formation events (Fig. 5, winter). The years when the WIW formation  
396 occurs, it is more homogeneously observed during the spring and summer  
397 seasons, mainly at station 25 at the Ibiza channel, but also at station 33 at  
398 the Mallorca channel when the WIW is advected with the Northern Current  
399 from its origin. This behaviour is smoothed in Fig. 5 (spring and summer)  
400 due to the averaging of the years with WIW formation and years with WIW  
401 absence. During the autumn the recently formed WIW is not present in the  
402 area (Fig. 5, autumn). Maximum AOU values related with the LIW core,  
403 from 400 dbar to 600 dbar, appear to increase  $\approx 0.1 \text{ ml l}^{-1}$  from spring to  
404 winter. Below the LIW an expected AOU decrease is seen with the depth  
405 corresponding to the more recent formation of the WMDW.

#### 406 *4.3. Deep water advection around the Balearic Islands*

407 The horizontal sections seen in Fig. 6 reveal that during December 2009,  
408 the north DO values are around  $0.1$  to  $0.2 \text{ ml l}^{-1}$ , higher than the south  
409 values both at 400 m depth (Fig. 6A) and 800 m depth (Fig. 6B). During  
410 June 2010, the north and south DO values are comparable at 400 m depth  
411 (Fig. 6C) but at 800 m depth (Fig. 6D) they are again  $0.15 \text{ ml l}^{-1}$  higher in  
412 the north. There is a north-south difference in the DO values at 800 m depth,  
413 both during December 2009 and June 2010, already been discussed prior in  
414 terms of deep water advection (Fig. 4 Idea0204). The deep water produced in  
415 the winter during the deep convection events in the Gulf of Lions cannot cross

416 the Ibiza and Mallorca channels advected with the Northern Current because  
417 the channel sills are only 800 m and 700 m in depth, respectively. Therefore,  
418 it gets advected around the Balearic Islands with the Balearic Current along  
419 the continental slope. This advection is observed as a decrease of the DO in  
420 the deep waters from the north to the south of the Islands (Fig. 6 and Fig.  
421 4).

422 It has also been discussed how the absolute DO minimum is observed at  
423 the core of the LIW at around 400 m (Fig. 4) being  $O_2^S \approx 66\%$  constant  
424 during the three Idea campaigns (Table 3). In those cases it was argued  
425 that this is probably due to the very little oxygen consumption at these  
426 depths that makes the DO appear constant during the four months sampled.  
427 The case of December 2009 at 400 m (Fig. 6 A) does not concur with that  
428 argument because it shows a north-south difference at 400 m depth of more  
429 than  $0.2 \text{ ml l}^{-1}$  (Fig. 6A). This increase in the DO observed in the north of  
430 the sampling region can be explained in terms of an oceanic front that was  
431 detected during the survey from the surface down to 400 m depth. This front  
432 caused upward vertical velocities of  $6 \text{ m day}^{-1}$  (Balbín et al., 2012). These  
433 intense upward velocities brought the lower and DO richer waters up from  
434 down above.

#### 435 4.4. Seasonal evolution of apparent oxygen utilisation at Cape Palos

436 To better understand the seasonal evolutions of AOU at Cape Palos (sta-  
437 tions 143 and 144 in Fig. 2), the presence or absence of the different water  
438 masses must be examined throughout the year and, in particular, the depths  
439 they occupy. The annual cycle of seasonal thermocline formation and col-  
440 lapse is clearly observed in Fig. 7. Isopycnals shallower than  $28.6 \text{ kg m}^{-3}$

441 begin to descend during the spring, reaching their maximum depth in the  
442 autumn and ascend, outcropping even the surface, during winter. The isopy-  
443 cnal  $28.0 \text{ kg m}^{-3}$  occasionally ventilates at the end of the winter, as in 2010.  
444 Subsurface waters display the spring-summer oxygen supersaturation (AOU  
445 below  $0 \text{ ml l}^{-1}$ ) due to the photosynthetic activity in the DCM within the  
446 thermocline.

447 Using the temperature and salinity patterns it is possible to observe the  
448 presence of WIW, with  $\theta \leq 13 \text{ }^\circ\text{C}$  and  $S \geq 38.3$  (Table 1). From the data  
449 at stations 25 and 16 (Balbín et al., 2013) it is evident that the WIW was  
450 present in the Ibiza channel every year, except 2007, although its presence  
451 was observed at Cape Palos only during 2009, 2010 and 2011 (Fig. 7). In  
452 2009 and 2011, the WIW was advected by the Northern Current, across the  
453 Ibiza channel, arriving at Cape Palos during the spring and summer. During  
454 the winter of 2010, the WIW formation was observed as far to the south as  
455 Cape Palos (Vargas-Yáñez et al., 2012). This fact is noted clearly in the  
456 temperature pattern of Fig. 7 which shows the higher volume occupied by  
457 the WIW during 2010, which appeared during the early winter that year.  
458 The events producing the WIW formation lead to even stronger ventilation,  
459 which is observed as the relative AOU minima  $\approx 0.4 - 0.6 \text{ ml l}^{-1}$  for the years  
460 2009, 2010 and 2011 (Fig. 7).

461 The depth of the interface with the LIW,  $S \geq 38.40$ , deepens during the  
462 spring and summer (earlier in 2010) when the recently formed WIW spreads  
463 over the LIW (Fig. 7). If the AOU is used as a water mass tracer, it can be  
464 deduced that the LIW core is associated with the  $\text{AOU} \geq 1.8 \text{ ml l}^{-1}$ . Using  
465 the AOU it is possible to observe the intermittent presence or absence of the

466 LIW cores that are observed at Cape Palos usually during the autumn and  
467 winter. The nucleus of the LIW can be observed intermittently at around  
468 400 to 500 dbar as the salinity maxima and AOU minima in Fig. 8.

469 The interphase between the LIW and WMDW can be defined by the  
470 38.48 isohaline and 12.9 °C isothermal around or below 1000 dbar in Fig.  
471 8. The depth of this interphase oscillates with time without a clear seasonal  
472 behaviour. The AOU and density patterns of Fig. 8 are well correlated in  
473 the deep waters, indicating that the denser waters are more ventilated and  
474 therefore more recent.

475 At around 1500 dbar it became possible to observe the indications of  
476 the thermohaline anomaly in the WMDW which appeared in 2005 (López-  
477 Jurado et al., 2005). This anomaly was due to the exceptional amount of  
478 DW formed during the 2005 winter and its causes are still unclear. Major  
479 changes observed in the western Mediterranean deep water include an abrupt  
480 increase in the deep heat and salt contents, when the isopycnals were lifted  
481 up hundreds of metres accompanied by the appearance of a sharp inversion  
482 in the  $\theta - S$  diagrams (Schroeder et al., 2012). This inversion in  $\theta$  and  $S$  can  
483 be observed as the relative maxima at  $\approx 1500$  dbar in Fig. 8. Those relative  
484 maxima in  $\theta$  and  $S$  appear intermittently every year. Their relatively higher  
485 AOU  $\approx 1.4 - 1.6 \text{ ml l}^{-1}$ , indicate that those waters are older than the deeper  
486 ones.

#### 487 4.5. Seasonal evolution of dissolved oxygen of biological origin

488 It is interesting to know the timing and progress of the DO of biological  
489 origin because the annual cycle is a dominant mode of variability in the bi-  
490 ology and chemistry of the ocean (Najjar and Keeling, 1997). In Fig. 9 the

491 annual cycles of  $O_2^S$  and fluorescence around the Balearic Islands are seen.  
492 The fluorescence data helps to visualise the seasonal cycle of the euphotic  
493 depth, driven by the solar flux at the surface, so that it is at its greatest in  
494 the early summer and its least in winter. The fluorescence signal starts to  
495 become well defined in early spring, occupying the whole photic layer. The  
496 signal deepens during the spring and early summer and ascends during the  
497 late summer and autumn. Around April the surface fluorescence vanishes,  
498 probably due to the depletion of the surface nutrients, and an intense subsur-  
499 face maximum appears. The  $O_2^S$  data shows that the oxygen within the mixed  
500 layer is close to the saturation concentration. Supersaturation is observed in  
501 the summer when the net community production is higher. In the waters be-  
502 low the mixed layer, the photosynthetically produced oxygen cannot escape  
503 to the atmosphere due to the strong stratification within the seasonal ther-  
504 mocline. This results in the subsurface oxygen supersaturation observed in  
505 the data between June and October. The supersaturation vanishes when the  
506 winter atmospheric forcing breaks the stratification and deepens the mixed  
507 layer, which leads to oxygen concentrations close to saturation. Maximum  
508  $O_2^S$  are always observed slightly above the subsurface fluorescence maximum.

## 509 5. Conclusions

510 To our knowledge there are very few published results on the DO char-  
511 acteristics around the Balearic Islands except for the work of Deya-Serra  
512 (1978). Manca et al. (2004) have done a climatological description of the DO  
513 on the Gulf of Lions while there are also some data collections close to the  
514 Balearic Islands (Miller, 1970) and several works on the OMZ of the Alboran

515 Sea (e.g. Packard et al., 1988). This, however, is the first work trying to  
516 make a characterisation on the DO considering all the information together,  
517 along the Spanish Mediterranean coast including the Balearic sub-basin, the  
518 Algerian sub-basin and the Alboran Sea.

519 The DO values observed around the Balearic Islands are in general con-  
520 currence with the prior climatology data as shown in Table 2 (Manca et al.,  
521 2004) and the earlier studies (Miller, 1970) except for the minimum DO val-  
522 ues observed within the LIW cores and the relative maximum related with  
523 the WIW. The surface DO values oscillate between  $6 \text{ ml l}^{-1}$  in winter and  
524  $4.5 \text{ ml l}^{-1}$  in summer. In spring and summer a subsurface oxygen supersat-  
525 uration due to biological activity is noted up to  $6$  to  $7 \text{ ml l}^{-1}$ . The relative  
526 maxima of the DO at 150 dbar are observed from winter until summer in  
527 the Ibiza and Mallorca channel related to WIW recently formed. The mini-  
528 mum DO values related to the LIW core, from 400 dbar to 600 dbar, appear  
529 to decrease from spring until winter, staying below  $4.0 \text{ ml l}^{-1}$  around the  
530 Balearic Islands. Below the LIW the expected DO increase with depth is  
531 seen, corresponding to the more recent formation of the deep waters.

532 The interannual variability accounts for unusual minima DO concentra-  
533 tions in the LIW, and minimum DO values below those reported by Packard  
534 et al. (1988) in the Alboran Sea OMZ. More data regarding DO measure-  
535 ments as well as on the nutrients and atmospheric variations are needed to  
536 clarify the reason for the DO observed in the Alboran Sea.

537 The DO concentrations and AOU are good indicators to detect the events  
538 of WIW and WMDW formation and their advection along the continental  
539 slope. The LIW and WMDW DO concentrations decrease along their path



540 due to biochemical consumption. Using the arguments of oxygen consump-  
541 tion it is possible to qualitatively show that the WIW propagates southwards  
542 with the Northern Current, mainly across the Ibiza Channel and the WMDW  
543 circulates with the Balearic Current, following an along-slope path around  
544 the Balearic Islands, requiring a longer time to arrive to the south of the  
545 islands. Accordingly, the DO concentrations below 800 m are 0.15 to 0.20  
546 ml l<sup>-1</sup> higher in the north of the Balearic Islands than in the south, and this  
547 difference is better observed in the winter.

548 It is possible to characterise the seasonal evolution of the different wa-  
549 ter masses and their AOU cycle in a station at Cape Palos. The seasonal  
550 thermocline formation and collapse are observed in the surface waters, while  
551 the sub-surface waters show the spring-summer oxygen supersaturation due  
552 to photosynthetic activity. Some of the years show the WIW (with its as-  
553 sociated AOU relative minimum) appearing intermittently above the LIW  
554 (with its associated AOU maximum), occupying its volume, during spring  
555 and summer. During 2010, the WIW appears earlier because it was excep-  
556 tionally formed as far to the south as Cape Palos (Vargas-Yáñez et al., 2012).  
557 The depth of the interphase between the LIW and WMDW varies with time.  
558 More sampling is warranted to characterise its seasonal behaviour. The AOU  
559 and density patterns indicate that both are correlated at the deep waters in-  
560 dicating that the denser waters are more recent. At 1500 dbar it is possible  
561 to observe the signals of the thermohaline anomaly in the WMDW (López-  
562 Jurado et al., 2005) in the potential temperature and salinity, that are yearly  
563 intermittent. Their relatively higher AOU indicate that those waters are  
564 older than the deeper ones.

565        Around the Balearic Islands the subsurface fluorescence maximum depth  
566 follows the seasonal cycle of the euphotic depth and vanishes in winter. Max-  
567 imum  $O_2^S$  are always observed slightly above the subsurface fluorescence max-  
568 imum.

### 569 **Acknowledgements**

570        We would like to render our sincere thanks to Dr. Biel Moya (UIB) for his  
571 careful reading of the manuscript and his useful comments. Data from the  
572 IBAMar database (Aparicio et al., 2012) was used when required. This work  
573 was partially supported by the TUNIBAL, CIRBAL and RADMED projects  
574 (funded by the IEO), and by the TUNIBAL-DOS project (REN2003-01176;  
575 CTM2004-20944E), BALEARES project (CTM2008-00478; CTM2009-07944),  
576 IDEA project (REN2002-04535-C02-02/MAR, REN2002-10670-E/MAR) and  
577 IDEADOS project (CTM2008-04489-C03-01) funded by the Spanish Ministry  
578 of Science and Innovation.

579 **References**580 **References**

581 Alemany, F., Quintanilla, L., Velez-Belchí, P., García, A., Cortés, D.,  
582 Rodríguez, J.M., Fernández de Puelles, M.L., González-Pola, C., López-  
583 Jurado, J.L., 2010. Characterization of the spawning habitat of Atlantic  
584 bluefin tuna and related species in the Balearic Sea (western Mediter-  
585 ranean). *Progress in Oceanography* 86, 21–38.

586 Amengual, T., Aparicio, A., Balbín, R., Fernández de Puelles, M., García-  
587 Martínez, M., Gaza, M., Jansá, J., Lopez-Jurado, J., Morillas, A., Moya,  
588 F., Plaza, F., Serra, M., Tel, E., Vargas-Yáñez, M., Vicente, L., Zunino,  
589 P., Álvarez, M., Bange, H., 2010. Implementing a multidisciplinary moni-  
590 toring system in the Spanish Mediterranean, in: 39th CIESM, CIESM The  
591 Mediterranean Science Commission. The Mediterranean Science Commis-  
592 sion, Venecia.

593 Amores, A., Monserrat, S., Marcos, M., 2013. Vertical structure and tempo-  
594 ral evolution of an anticyclonic eddy in the Balearic Sea (Western Mediter-  
595 ranean). *Journal of Geophysical Research: Oceans* .

596 Aparicio, A., López-Jurado, J., Balbín, R., Jansá, J., Amengual, B., 2012.  
597 IBAMar 2.0: 36 years sampling on the Western Mediterranean Sea, in:  
598 EGU General Assembly Conference Abstracts, p. 8476.

599 Balbín, R., Flexas, M., López-Jurado, J., Peña, M., Amores, A., Alemany,  
600 F., 2012. Vertical velocities and biological consequences at a front detected  
601 at the Balearic Sea. *Continental Shelf Research* 47, 28–41.

- 602 Balbín, R., López-Jurado, J.L., Flexas, M.M., Reglero, P., Vélez-Velchí, P.,  
603 González-Pola, C., Rodríguez, J.M., García, A., Alemany, F., 2013. In-  
604 terannual variability of the early summer circulation around the Balearic  
605 Islands: driving factors and potential effects on the marine ecosystem.  
606 *Journal of Marine Systems* , –.
- 607 Bethoux, J., 1989. Oxygen consumption, new production, vertical advection  
608 and environmental evolution in the Mediterranean Sea. *Deep Sea Research*  
609 *Part A. Oceanographic Research Papers* 36, 769–781.
- 610 Chester, R., 2000. *Marine geochemistry*. Wiley-Blackwell.
- 611 Cullen, J.J., 1982. The deep chlorophyll maximum: comparing vertical pro-  
612 files of chlorophyll a. *Canadian Journal of Fisheries and Aquatic Sciences*  
613 39, 791–803.
- 614 Deya-Serra, M.M., 1978. Datos sobre la distribución del oxígeno disuelto y  
615 nutrientes en aguas próximas a la isla de Mallorca. volume 246. Instituto  
616 Español de Oceanografía.
- 617 Diaz, R., Rosenberg, R., 2008. Spreading dead zones and consequences for  
618 marine ecosystems. *science* 321, 926.
- 619 Estrada, M., 1996. Primary production in the northwestern mediterranean.  
620 *Scientia Marina* 60, 55–64.
- 621 Font, J., 1987. The path of the levantine intermediate water to the alboran  
622 sea. *Deep Sea Research Part A. Oceanographic Research Papers* 34, 1745–  
623 1755.

- 624 Garcia, Gordon, 1993. Oxygen solubility in seawater: Better fitting equa-  
625 tions. *Limnology and Oceanography* 38, 656–656.
- 626 Garcia, H., Locarnini, R., Boyer, T., Antonov, J., 2006. World Ocean Atlas  
627 2005. Vol. 3, Dissolved oxygen, apparent oxygen utilization, and oxygen  
628 saturation. Ed. NOAA Atlas NESDIS 63, U.S., Government Printing Of-  
629 fice, Washington, D.C.
- 630 Hopkins, T., 1978. Physical processes in the Mediterranean basins. *Estuarine*  
631 *Transport Processes* , 269–310.
- 632 Jenkins, W., 1987.  $^3\text{H}$  and  $^3\text{He}$  in the Beta Triangle: Observations of  
633 Gyre ventilation and oxygen utilization rates. *J. Phys. Oceanogr.*;(United  
634 States) 17.
- 635 López-García, M., Millot, C., Font, J., García-Ladona, E., 1994. Surface  
636 circulation variability in the Balearic Basin. *Journal of geophysical research*  
637 99, 3285–3296.
- 638 López-Jurado, J.L., González-Pola, C., Vélez-Belchí, P., 2005. Observation  
639 of an abrupt disruption of the long-term warming trend at the Balearic  
640 Sea, western Mediterranean Sea, in summer 2005. *Geophysical Research*  
641 *Letters* 32.
- 642 López-Jurado, J.L., Marcos, M., Monserrat, S., 2008. Hydrographic condi-  
643 tions affecting two fishing grounds of Mallorca island (Western Mediter-  
644 ranean): during the IDEA Project (2003-2004). *Journal of Marine Systems*  
645 71, 303–315.

- 646 Manca, B., Burca, M., Giorgetti, A., Coatanoan, C., Garcia, M., Iona, A.,  
647 2004. Physical and biochemical averaged vertical profiles in the Mediter-  
648 ranean regions: an important tool to trace the climatology of water masses  
649 and to validate incoming data from operational oceanography. *Journal of*  
650 *marine systems* 48, 83–116.
- 651 Massutí, E., Olivar, M.P., Monserrat, S., Rueda, L., Oliver, P., 2013. To-  
652 wards the understanding of the influence of the environmental conditions  
653 on the demersal resources and ecosystems in the western Mediterranean:  
654 Motivations, aims and methods of the IDEADOS project. submitted to  
655 *Journal of Marine Systems* .
- 656 MEDOC-Group, 1970. Observation of formation of deep water in the  
657 Mediterranean Sea. *Nature* 227, 1040.
- 658 Miller, A., 1970. *Mediterranean Sea Atlas of Temperature, Salinity, and*  
659 *Oxygen. Profiles and Data from Cruises of RV Atlantis and RV Chain.*  
660 *Technical Report. Woods Hole Oceanographic Institution. Massachusetts.*
- 661 Millot, C., Taupier-Letage, I., 2005. Additional evidence of low entrainment  
662 across the algerian subbasin by mesoscale eddies and not by a permanent  
663 westward flow. *Progress in Oceanography* 66, 231–250.
- 664 Najjar, R., Keeling, R., 1997. Analysis of the mean annual cycle of the  
665 dissolved oxygen anomaly in the world ocean. *Journal of marine research*  
666 55, 117–151.
- 667 Nykjaer, L., et al., 2009. Mediterranean sea surface warming 1985-2006.  
668 *Climate research (Open Access for articles 4 years old and older)* 39, 11.

- 669 Packard, T., Minas, H., Coste, B., Martinez, R., Bonin, M., Gostan, J.,  
670 Garfield, P., Christensen, J., Dortch, Q., Minas, M., et al., 1988. Forma-  
671 tion of the Alboran oxygen minimum zone. *Deep Sea Research Part A.*  
672 *Oceanographic Research Papers* 35, 1111–1118.
- 673 Pinot, J.M., López-Jurado, J.L., Riera, M., 2002. The CANALES experi-  
674 ment (1996-1998). Interannual, seasonal, and mesoscale variability of the  
675 circulation in the Balearic Channels. *Progress In Oceanography* 55, 335 –  
676 370.
- 677 SBE43, 2013. SBE 43 Dissolved Oxygen Sensor – Background Information,  
678 Deployment Recommendations, and Cleaning and Storage.
- 679 Schroeder, K., García-Lafuente, J., Josey, S.A., Artale, V., Nardelli, B.B.,  
680 Carrillo, A., Gacic, M., Gasparini, G.P., Herrmann, M., Lionello, P., Lud-  
681 wig, W., Millot, C., Ozsoy, E., Pisacane, G., Sánchez-Garrido, J.C., San-  
682 nino, G., Santoleri, R., Somot, S., Struglia, M., Stanev, E., Taupier-Letage,  
683 I., Tsimplis, M.N., Vargas-Yañez, M., Zervakis, V., Zodiatis, G., 2012. 3  
684 - Circulation of the Mediterranean Sea and its Variability, in: Lionello, P.  
685 (Ed.), *The Climate of the Mediterranean Region: From the Past to the*  
686 *Future*. Elsevier, Oxford, pp. 187 – 256.
- 687 Shaffer, G., Olsen, S., Pedersen, J., 2009. Long-term ocean oxygen depletion  
688 in response to carbon dioxide emissions from fossil fuels. *Nature Geoscience*  
689 2, 105–109.
- 690 Souvermezoglou, E., Krasakopoulou, E., et al., 2002. High oxygen consump-

- 691 tion rates in the deep layers of the North Aegean Sea (eastern Mediter-  
692 ranean). *Mediterranean Marine Science* 3, 55–64.
- 693 Stramma, L., Johnson, G.C., Sprintall, J., Mohrholz, V., 2008. Expanding  
694 oxygen-minimum zones in the tropical oceans. *Science* 320, 655–658.
- 695 Stratford, K., Williams, R., Drakopoulos, P., 1998. Estimating climatological  
696 age from a model-derived oxygen–age relationship in the mediterranean.  
697 *Journal of marine systems* 18, 215–226.
- 698 Strickland, J., Parsons, T., 1972. A practical handbook of seawater analysis.  
699 *Bull. Fish. Res. Board Can* 167.
- 700 Vargas-Yáñez, M., Zunino, P., Schroeder, K., López-Jurado, J., Plaza, F.,  
701 Serra, M., Castro, C., García-Martínez, M., Moya, F., Salat, J., 2012.  
702 Extreme Western Intermediate Water formation in winter 2010. *Journal*  
703 *of Marine Systems* 105-108, 52–59.



Water mass	Values at origin	Local values
AW	$15.0 < \theta < 18.0$	$15.0 < \theta < 28.0$
	$36.15 < S < 36.50$	$36.50 < S < 37.50$
Resident AW	$13.0 < \theta < 28.0$	$13.0 < \theta < 28.0$
	$37.50 < S < 38.30$	$37.50 < S < 38.20$
WIW	$12.5 < \theta < 13.0$	$12.5 < \theta < 13.0$
	$37.90 < S < 38.30$	$37.90 < S < 38.30$
LIW	$14.0 < \theta < 15.0$	$13.0 < \theta < 13.4$
	$38.70 < S < 38.80$	$38.45 < S < 38.60$
WMDW	$12.7 < \theta < 12.9$	$12.7 < \theta < 12.9$
	$38.40 < S < 38.48$	$38.40 < S < 38.48$

Table 1: Characteristic values of the potential temperature ( $\theta$ ) and salinity ( $S$ ) of the different water types and local values in the Balearic Sea (López-Jurado et al., 2008)

Water mass	Temperature (°C)	Salinity	Oxygen (ml l <sup>-1</sup> )
<i>Gulf of Lions</i>			
Surface water (0-5 m)	17.61±2.30 (14,218)	37.88±0.45 (9472)	5.44±0.24 (2182)
LIW (400 m)	13.17±0.11 (3101)	38.48±0.03 (2306)	4.48±0.17 (610)
WMDW (≥ 1500 m)	13.04±0.02 (3218)	38.42±0.01 (3473)	4.60±0.07 (1214)
<i>Alboran Sea</i>			
Surface water (0-5 m)	17.85±0.616 (18,874)	36.57±0.28 (7122)	5.44±0.33 (1877)
LIW (400 m)	13.07±0.08 (2014)	38.45±0.04 (1588)	4.21±0.17 (320)
WMDW (≥ 1500 m)	13.08±0.03 (176)	38.44±0.01 (170)	4.50±0.09 (21)

Table 2: Spatially averaged water properties in two regions of the Western Mediterranean according to Manca et al. (2004). The average and standard deviations for the physical parameters (the quantity of data used are indicated within brackets) for three layers, which essentially characterise the water column structure.

Campaign	Idea0204		Idea0404		Idea0604	
	O <sub>2</sub> <sup>S</sup>	AOU	O <sub>2</sub> <sup>S</sup>	AOU	O <sub>2</sub> <sup>S</sup>	AOU
Surface water (0-5 m)	98%	0.1	100%	0	100%	0
Surface water (50-80 m)	98%	0.1	100%	0	116%	-0.7
WIW (100-200 m)	98%	0.1	90%	0.6	85-87%	0.6-0.8
LIW (400-500 m)	67%	1.9	66%	1.9	67%	1.9
WMDW (≥ 1500 m)	70-72%	1.6-1.7	71%	1.7	71%	1.6

Table 3: A resume of the O<sub>2</sub><sup>S</sup> and AOU (ml l<sup>-1</sup>) values for the vertical profiles in Fig. 4.

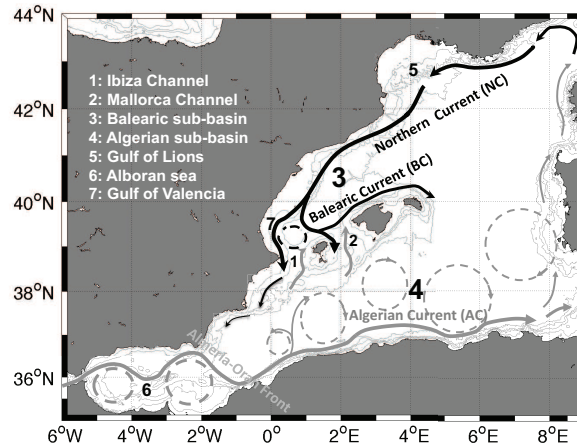


Figure 1: The Balearic Islands and the main surface currents that describe the regional circulation. The Mallorca and Ibiza channels are shown. The Northern and Balearic Currents are indicated by dark grey arrows while the Algerian gyres are indicated by light grey arrows. The light grey lines denote the isobaths (100 m, 500 m, 1000 m, and 2000 m).

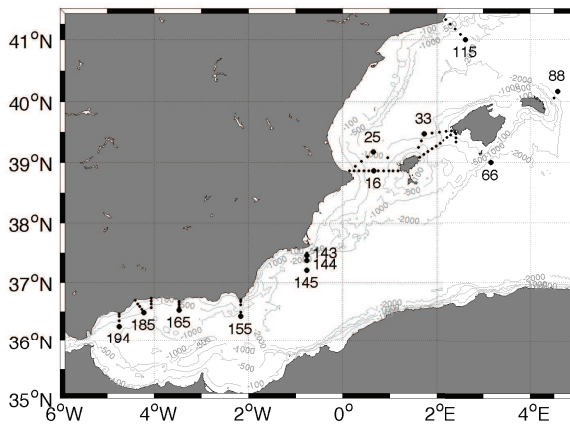


Figure 2: Distribution of the RADMED-1007 stations along the Spanish coast. Numbered black dots correspond to the stations selected for the present study.

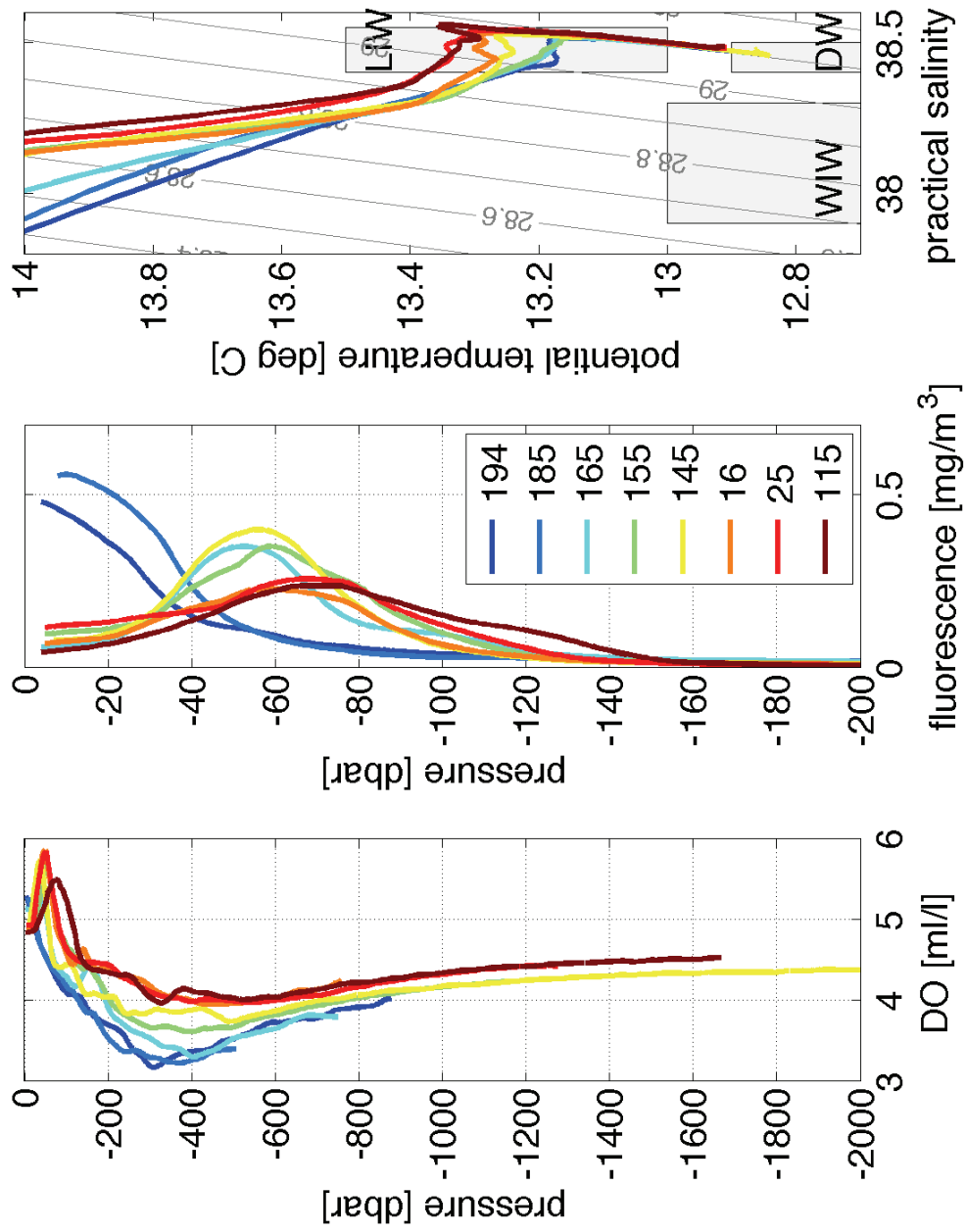


Figure 3: Vertical profiles of the DO from the surface to the bottom and fluorescence from the surface to 200 dbar at the stations along the mainland are shown in Fig. 2, with their corresponding  $\theta - S$  diagrams. The grey boxes over the  $\theta - S$  axis indicate the local values that characterise the different water masses as shown in Table 1.

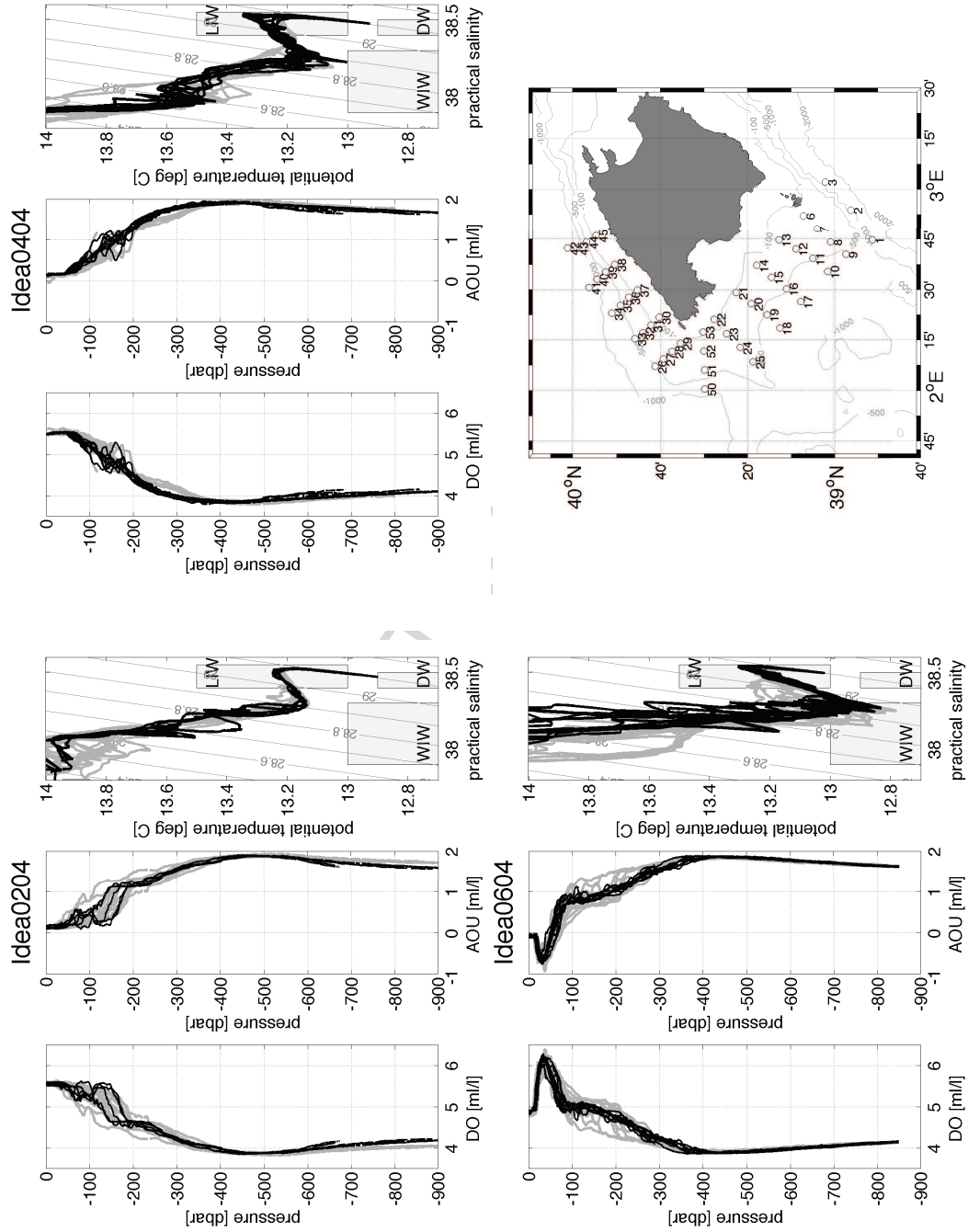


Figure 4: Vertical profiles of the DO and AOU from the surface to the bottom at the IDEA stations are shown in the map and corresponding to winter (February 2004), spring (April 2004) and summer (June 2004) and their corresponding  $\theta$ - $S$  diagrams. The black lines refer to stations 34 to 45, while the grey lines indicate stations 1 to 17 as shown in the map.

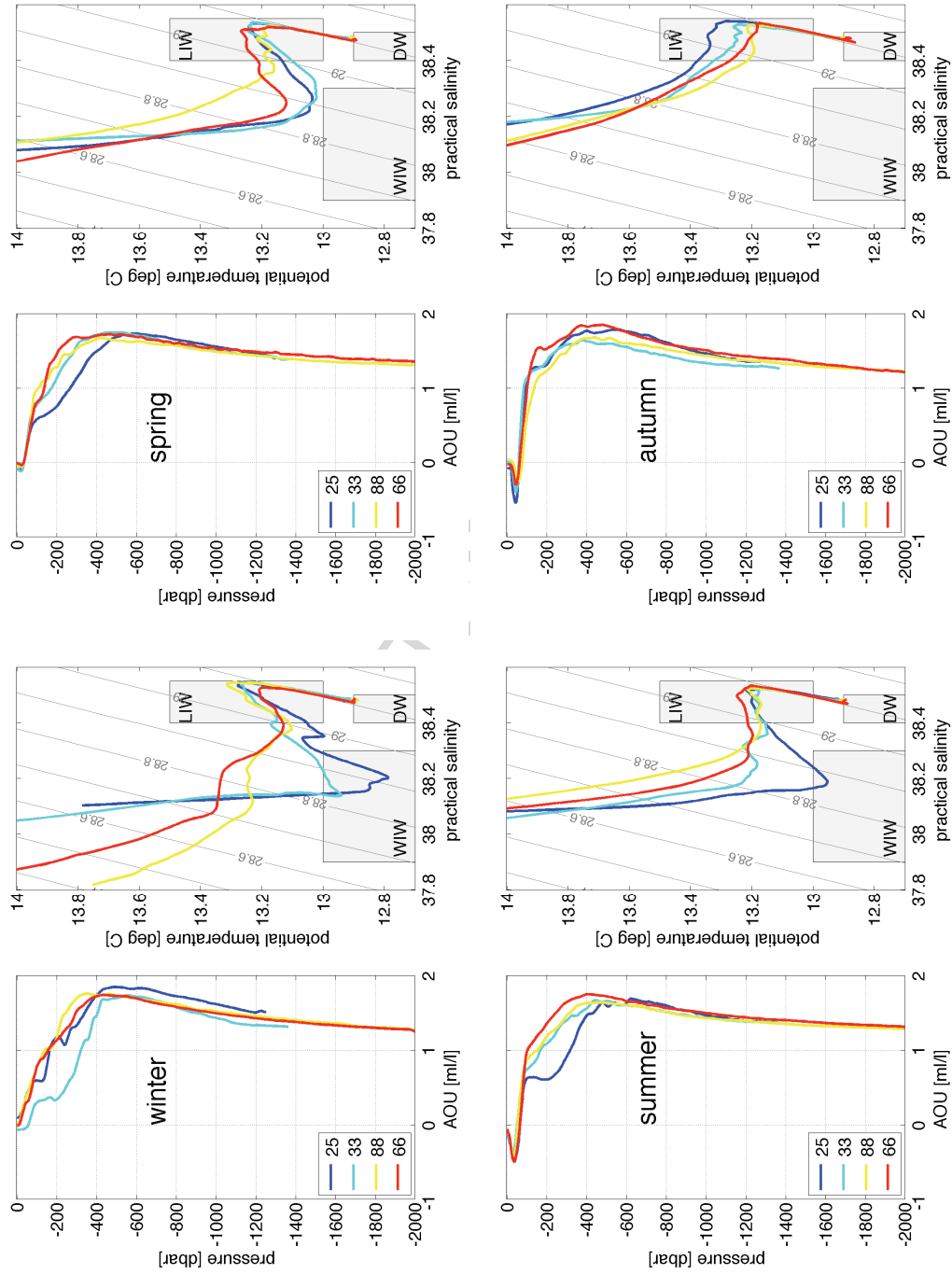


Figure 5: Vertical profiles of the AOU in  $\text{ml l}^{-1}$  from the surface to the bottom corresponding to the winter, spring, summer and autumn mean values at selected deep stations around the Balearic Islands and their corresponding  $\theta - S$  diagrams. Numbers 25 and 33 are stations in the Ibiza and Mallorca channels, respectively, while numbers 88 and 66 are the deep stations in the north of Menorca and south of Cabrera, as shown in Fig. 2.

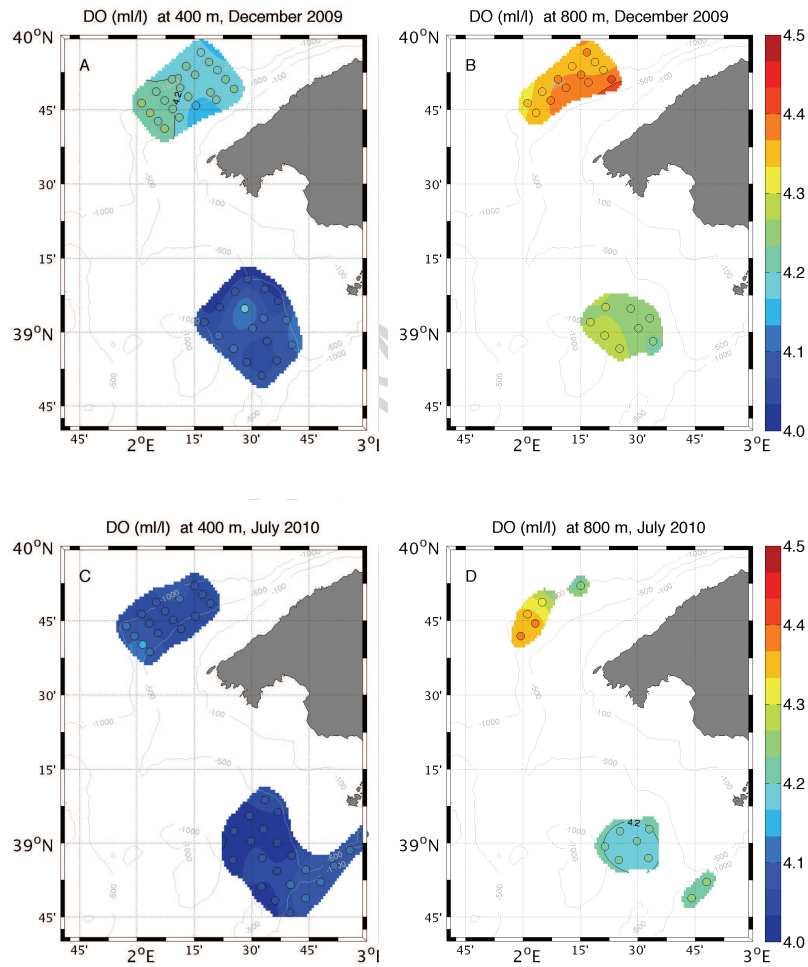
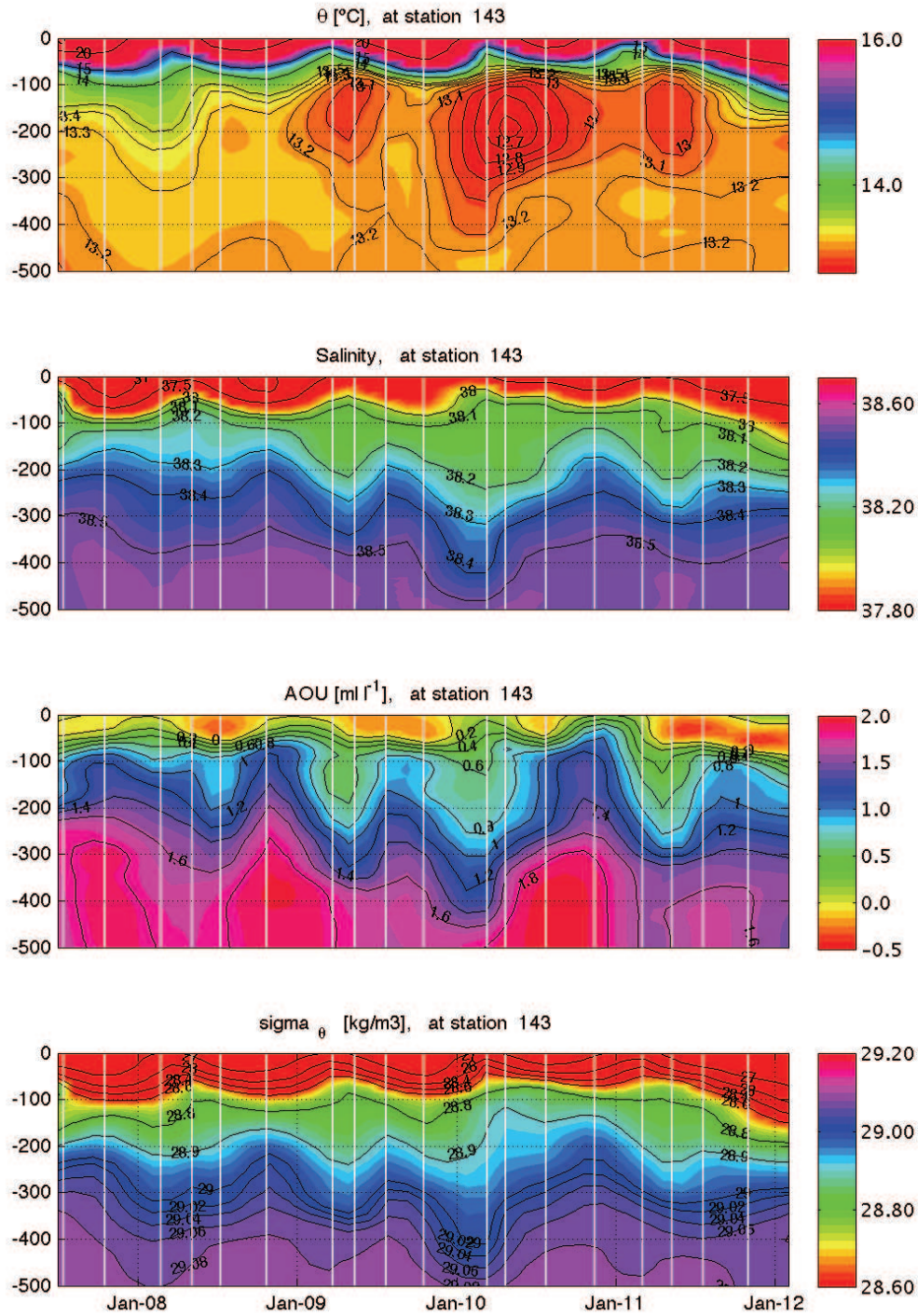


Figure 6: The DO at 400 m (A and C) and 800 m (B and D) for the IDEADOS surveys. A and B correspond to the early winter while C and D indicate the summer.



39  
 Figure 7: Temperature, salinity, AOU and  $\sigma_\theta$  at station 143 versus pressure and time. Grey vertical lines correspond to station sampling date.



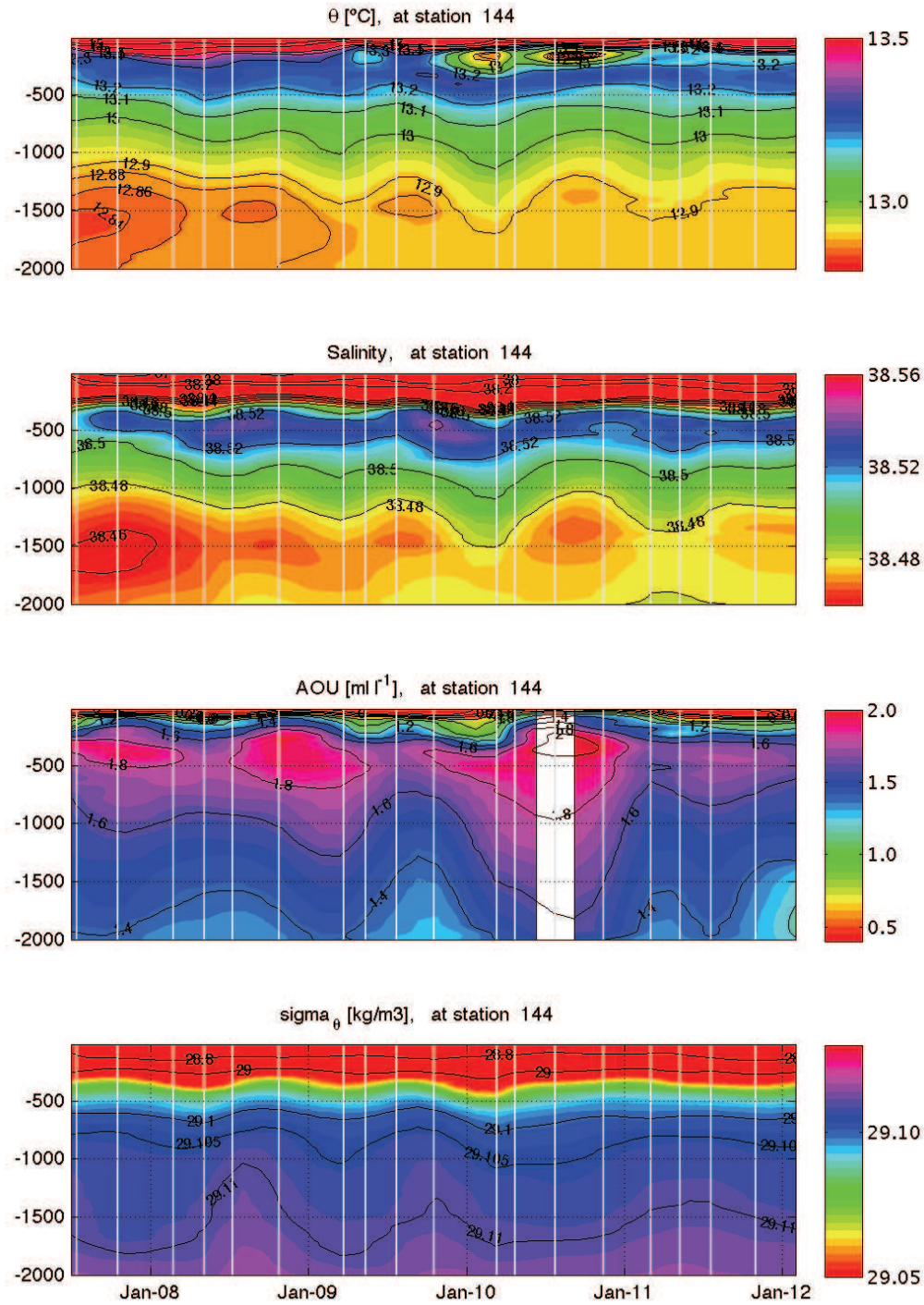


Figure 8: Temperature, salinity, AOU and  $\sigma_\theta$  at station 144 versus pressure and time. Grey vertical lines correspond to survey date. White box indicate there were not DO data.

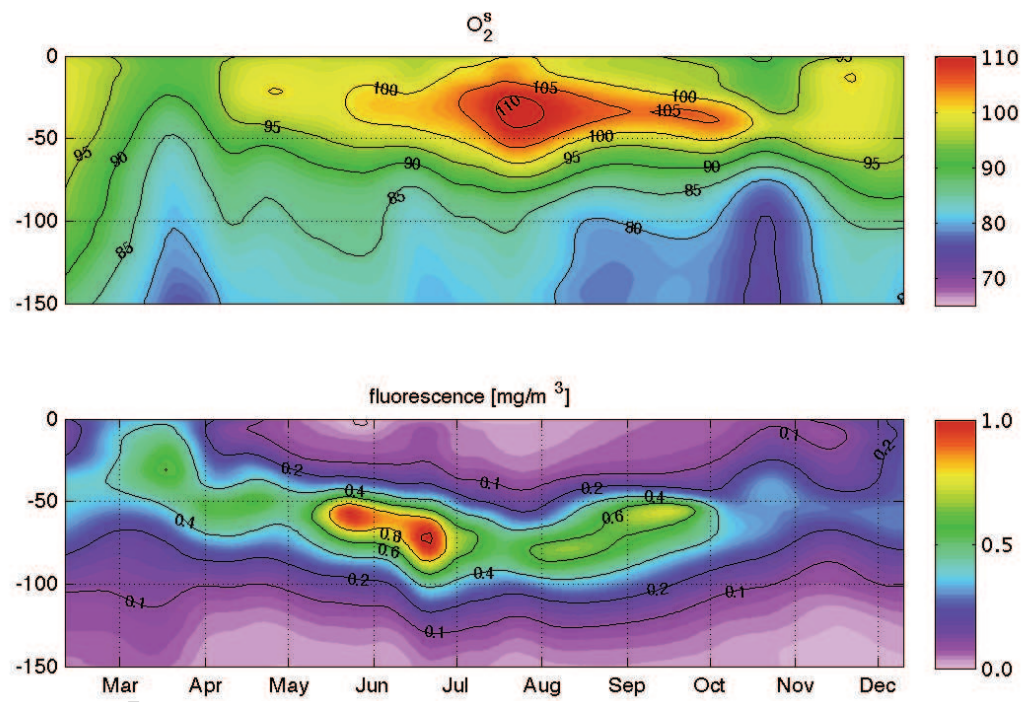


Figure 9: The  $O_2^s$  and fluorescence around the Balearic islands versus pressure and time.

**Highlights**

DO around the Balearic Islands are in agreement with the prior climatology data.

Minimum DO values are observed within the LIW and relative maximum within the WIW.

Maximum DO are always observed slightly above the subsurface fluorescent maximum.

DO is a indicator to WIW and WMDW formation and advection along continental slope.

The seasonal evolution of the different water masses and their AOU is described